Analysis and subgrid modeling of shock-wave/boundary-layer interaction

By N. A. Adams[1], S. Stolz[1], A. Honein AND K. Mahesh

This paper considers two different issues that arise in LES of supersonic wall bounded flows. First, an *a priori* analysis of subgrid-scale models in a highly compressible environment is conducted. DNS data from a Mach 3 compression-corner are used for this purpose. Models of the scale-similarity type correlate best with filtered DNS data. Lower correlations are obtained with the dynamic mixed model, the dynamic Smagorinsky model, and the fixed-coefficient Smagorinsky model. Second, the possibility of treating the shock as a subgrid scale is investigated. It is found that a straightforward application of dynamic eddy-viscosity models is unsuccessful. A direct deconvolution is found to give a proper agreement between a 6th order spectral-like finite-difference scheme and a 5th order ENO shock-capturing scheme for the simple case of a 1D convected $M = 3$ shock.

1. Introduction

Large-eddy simulation (LES) is now a viable tool for studying moderately complex turbulent flows at Reynolds numbers for which direct numerical simulation (DNS) is infeasible. Most LES performed have been in incompressible flows. This paper considers LES of a highly compressible flow – the interaction of a shock wave with a Mach 3 turbulent boundary layer along a compression corner. Two issues relevant to the LES of this flow are studied: the accuracy of subgrid models, and the effect of subgrid models on the shock, which itself can be a subgrid-scale entity.

In this paper we conduct an *a priori* analysis of DNS data for supersonic compression ramp flow. Several models are considered. Of particular concern are SGS terms in the energy equation, where compressibility effects are significant. Next, we briefly address the question of whether and how a shock can be treated as a subgrid-scale structure.

2. Part 1: Analysis of compression-corner data

In this section, we focus on *a priori* analysis of data from DNS of a compression ramp at $M = 3$, $Re_\theta = 1685$ and a deflection angle of 18°. The numerical method used in the DNS is described by Adams (1998; results are analyzed and reported by Adams & Kleiser (1998).

1 ETH Zürich, Institute of Fluid Dynamics, CH-8092 Zürich, Switzerland.

2.1 Mathematical model

Considering the conservative Navier-Stokes equations in curvilinear coordinates, we apply a filter operation with filter width Δ in computational space ξ to the dependent variables

$$\overline{\phi}(\xi) = G(\xi - \xi') \otimes \phi(\xi') = \int_\Omega G(\xi - \xi')\phi(\xi')d\xi' \quad .$$

We obtain the fundamental equations for the resolved conservative variables $\{\overline{\rho},\ \tilde{u}_i,\ \check{E}\}$. Favre-filtered quantities are denoted by "$\tilde{\bullet}$". They are computed from a mass-weighted filtering operation

$$\tilde{\phi} = \frac{\overline{\rho\phi}}{\overline{\rho}} \quad .$$

The nomenclature of the following equations may be found in Vreman (1995) and Adams (1998). The filtered continuity equation becomes

$$\tfrac{1}{J}\tfrac{\partial \bar{\rho}}{\partial t} + \tfrac{\partial}{\partial \xi_i}\left(\tfrac{\bar{\rho}\tilde{u}_j}{J}\tfrac{\partial \xi_i}{\partial x_j}\right) = \gamma_{C1} + \gamma_{C2}, \quad \text{where}$$

$$\begin{aligned} \gamma_{C1} &= \tfrac{\partial}{\partial \xi_k}\left(\overline{\tfrac{\rho u_j}{J}}\tfrac{\partial \xi_k}{\partial x_j}\right) - \tfrac{\partial}{\partial \xi_k}\left(\overline{\tfrac{\rho u_j}{J}\tfrac{\partial \xi_k}{\partial x_j}}\right) \\ \gamma_{C2} &= \tfrac{\partial}{\partial \xi_k}\left(\overline{\tfrac{\rho u_j}{J}}\tfrac{\partial \xi_k}{\partial x_j}\right) - \overline{\tfrac{\partial}{\partial \xi_k}\left(\tfrac{\rho u_j}{J}\tfrac{\partial \xi_k}{\partial x_j}\right)} \end{aligned} \quad . \tag{1}$$

γ_{C1} is an $\mathcal{O}(\Delta^2)$ error term, which results from the non-identity mapping between computational space ξ_i and physical space x_i. γ_{C2} is an error due to a variable filter width (commutation error). This error vanishes since in our case the filter G is not an explicit function of ξ_i and filtering is peformed in computational space.

The filtered momentum equations are

$$\begin{aligned} \tfrac{1}{J}\tfrac{\partial \bar{\rho}\tilde{u}_i}{\partial t} + \tfrac{\partial}{\partial \xi_k}\left(\tfrac{\bar{\rho}\tilde{u}_i\tilde{u}_j}{J}\tfrac{\partial \xi_k}{\partial x_j} + \tfrac{\bar{p}}{J}\delta_{ij}\tfrac{\partial \xi_k}{\partial x_j}\right) - \tfrac{\partial}{\partial \xi_k}\left(\tfrac{\check{\sigma}_{ij}}{J}\tfrac{\partial \xi_k}{\partial x_j}\right) = \\ = -\tfrac{\partial}{\partial \xi_k}\left(\tfrac{\bar{\rho}\tau_{ij}}{J}\tfrac{\partial \xi_k}{\partial x_j}\right) + \beta_i + \gamma_{I1i} + \gamma_{I2i} \end{aligned}$$

$$\begin{aligned} \bar{\rho}\tau_{ij} &= \bar{\rho}(\widetilde{u_i u_j} - \tilde{u}_i\tilde{u}_j) \\ \sigma_{ij} &= \tfrac{\mu}{Re}S_{ij} \\ S_{ij} &= \tfrac{\partial \xi_k}{\partial x_j}\tfrac{\partial u_i}{\partial \xi_k} + \tfrac{\partial \xi_k}{\partial x_i}\tfrac{\partial u_j}{\partial \xi_k} - \tfrac{2}{3}\tfrac{\partial \xi_k}{\partial x_l}\tfrac{\partial u_l}{\partial \xi_k}\delta_{ij} \\ \beta_i &= \tfrac{\partial}{\partial \xi_k}\left(\tfrac{\bar{\sigma}_{ij} - \check{\sigma}_{ij}}{J}\tfrac{\partial \xi_k}{\partial x_j}\right) \end{aligned} \quad . \tag{2}$$

$$\begin{aligned} \gamma_{I1i} &= \tfrac{\partial}{\partial \xi_k}\left(\overline{\tfrac{\rho u_i u_j + p\delta_{ij} - \sigma_{ij}}{J}}\tfrac{\partial \xi_k}{\partial x_j}\right) - \tfrac{\partial}{\partial \xi_k}\left(\overline{\tfrac{\rho u_i u_j + p\delta_{ij} - \sigma_{ij}}{J}\tfrac{\partial \xi_k}{\partial x_j}}\right) \\ \gamma_{I2i} &= \tfrac{\partial}{\partial \xi_k}\left(\overline{\tfrac{\rho u_i u_j + p\delta_{ij} - \sigma_{ij}}{J}}\tfrac{\partial \xi_k}{\partial x_j}\right) - \overline{\tfrac{\partial}{\partial \xi_k}\left(\tfrac{\rho u_i u_j + p\delta_{ij} - \sigma_{ij}}{J}\tfrac{\partial \xi_k}{\partial x_j}\right)} \end{aligned}$$

The term β_i arises from the non-linearity of the viscous stresses. γ_{I1} and γ_{I2} are error terms analogous to γ_{C1} and γ_{C2}.

The resolved-energy equation is obtained by filtering the enthalpy equation and by adding the filtered momentum equation, multiplied by $\tilde{u}_i$:

$$\begin{gathered}\frac{1}{J}\frac{\partial \check{E}}{\partial t}+\frac{\partial}{\partial \xi_k}\left(\frac{\check{E}+\bar{p}}{J}\tilde{u}_j\frac{\partial \xi_k}{\partial x_j}\right)-\frac{\partial}{\partial \xi_k}\left(\frac{\check{\sigma}_{ij}\tilde{u}_i}{J}\frac{\partial \xi_k}{\partial x_j}\right)+\frac{\partial}{\partial \xi_k}\left(\frac{\check{q}_j}{J}\frac{\partial \xi_k}{\partial x_j}\right)= \\ =-\alpha_1-\alpha_2-\alpha_3+\alpha_4+\alpha_5-\alpha_6+\gamma_{E1}+\gamma_{E2}\end{gathered}$$

$$\begin{aligned}q_j &= \frac{\mu}{(\gamma-1)RePrM^2}\frac{\partial \xi_k}{\partial x_j}\frac{\partial T}{\partial \xi_k} \\ \alpha_1 &= \tilde{u}_i\frac{\partial}{\partial \xi_k}\left(\frac{\bar{p}\tau_{ij}}{J}\frac{\partial \xi_k}{\partial x_j}\right) \\ \alpha_2 &= \frac{1}{\gamma-1}\frac{\partial}{\partial \xi_k}\left(\frac{\overline{pu_j}-\bar{p}\tilde{u}_j}{J}\frac{\partial \xi_k}{\partial x_j}\right) \\ \alpha_3 &= \frac{1}{J}\left(\overline{p\frac{\partial u_j}{\partial \xi_k}}-\bar{p}\frac{\partial \tilde{u}_j}{\partial \xi_k}\right)\frac{\partial \xi_k}{\partial x_j} \\ \alpha_4 &= \frac{1}{J}\left(\overline{\sigma_{ij}\frac{\partial u_i}{\partial \xi_k}}-\bar{\sigma}_{ij}\frac{\partial \tilde{u}_i}{\partial \xi_k}\right)\frac{\partial \xi_k}{\partial x_j} \\ \alpha_5 &= \frac{\partial}{\partial \xi_k}\left(\frac{\tilde{u}_i\bar{\sigma}_{ij}-\tilde{u}_i\check{\sigma}_{ij}}{J}\frac{\partial \xi_k}{\partial x_j}\right) \\ \alpha_6 &= \frac{\partial}{\partial \xi_k}\left(\frac{\bar{q}_j-\check{q}_j}{J}\frac{\partial \xi_k}{\partial x_j}\right)\end{aligned} \quad . \qquad (3)$$

$$\begin{gathered}\gamma_{H1}=\frac{\partial}{\partial \xi_k}\left[\left(\overline{\frac{pu_j}{\gamma-1}}+q_j\right)\frac{1}{J}\frac{\partial \xi_k}{\partial x_j}\right]-\frac{\partial}{\partial \xi_k}\left[\overline{\left(\frac{pu_j}{\gamma-1}+q_j\right)\frac{1}{J}\frac{\partial \xi_k}{\partial x_j}}\right]+\frac{1}{J}\overline{p\frac{\partial u_j}{\partial \xi_k}}\frac{\partial \xi_k}{\partial x_j}- \\ -\overline{\frac{p}{J}\frac{\partial u_j}{\partial \xi_k}\frac{\partial \xi_k}{\partial x_j}}+\overline{\frac{\sigma_{ij}}{J}\frac{\partial u_i}{\partial \xi_k}\frac{\partial \xi_k}{\partial x_j}}-\frac{1}{J}\overline{\sigma_{ij}\frac{\partial u_i}{\partial \xi_k}}\frac{\partial \xi_k}{\partial x_j}\end{gathered}$$

$$\gamma_{H2}=\frac{\partial}{\partial \xi_k}\left[\overline{\left(\frac{pu_j}{\gamma-1}+q_j\right)\frac{1}{J}\frac{\partial \xi_k}{\partial x_j}}\right]-\overline{\frac{\partial}{\partial \xi_k}\left[\left(\frac{pu_j}{\gamma-1}+q_j\right)\frac{1}{J}\frac{\partial \xi_k}{\partial x_j}\right]}$$

$$\gamma_{E1}=\tilde{u}_i\gamma_{I1i}+\gamma_{H1}$$

$$\gamma_{E2}=\tilde{u}_i\gamma_{I2i}+\gamma_{H2}$$

A "$\check{\bullet}$" indicates that the respective quantities are computed according to their definition but with resolved primitive variables, e.g., $\check{E}=\bar{p}/(\gamma-1)+\underline{\bar{\rho}\tilde{u}_i\tilde{u}_i/2,}$ which we call the total resolved energy. Note that the filtered Jacobian $\underline{\partial \xi_i/\partial x_j}$ has been replaced by the unfiltered $\partial \xi_i/\partial x_j$. This contributes another error of order $\mathcal{O}(\Delta^2)$, which is on the order of the leading error terms. Whereas subgrid-scale stresses formally are analogous to the incompressible case, additional terms appear in Eqs. (1) - (3) due to the non-vanishing velocity-field divergence and due to variable viscosity. Some of these additional subgrid-scale terms have an intuitive physical interpretation as shown in Table 1.

$SGS-term$	physical interpretation
α_1	SGS-dissipation.
α_2	Pressure-velocity correlation; reversible transfer between internal and kinetic energy; by rearrangement an expression similar to the turbulent heat flux in RANS-modeling is found: $\alpha_2 = \frac{1}{(\gamma-1)\gamma M^2}\frac{\partial}{\partial\xi_k}\left(\frac{\overline{\rho T u_j}-\bar{\rho}\tilde{T}\tilde{u}_j}{J}\frac{\partial\xi_k}{\partial x_j}\right)$.
α_3	Pressure-dilatation correlation.
α_4	SGS-molecular dissipation.

TABLE 1. Physical interpretation of SGS-terms.

2.2 A priori analysis

For an assessment of the correlation between modeled and exact data, an *a priori* analysis of a DNS data base for a turbulent supersonic compression ramp (Adams and Kleiser, 1998) was performed. The filter used here is a Padé filter of 2nd order (Lele, 1992) where the advantage of having a continuous parameter to change the effective filter width is used to tune the filter in order to best approximate a Gauß transfer function in wavenumber space. The cut-off wavenumber is $k_c = \pi/4$ for the *grid filter* and $k_c' = \pi/8$ for the *test filter* where required. The filter formula is

$$\alpha\bar{f}_{i-1} + \bar{f}_i + \alpha\bar{f}_{i+1} = af_i + \frac{b}{2}(f_{i-1} + f_{i+1}) \tag{4}$$

where $b = a = 1/2 + \alpha$. The effective cutoff wavenumber is given by Δ in the exact Gauß transfer function

$$\hat{G}(\xi) = \mathrm{e}^{-(\Delta\xi/2)^2/8}$$

where ξ is the wavenumber normalized with the grid-spacing h. By approximating the Gauß transfer function by the transfer function of filter (4), one finds the best matches for $\alpha = -0.2$ for an effective filter width $\Delta = 4h$ and $\alpha = -0.43$ for an effective filter width $\Delta = 8h$.

We refer to three different subdomains of the compression corner geometry, the locations of which are indicated in Fig. 1. The first (A) is located ahead of the shock, the second (B) around the corner, and the last (C) behind the shock. All blocks span the domain in y-direction. The streamwise extent of block A is about 2.7 mean-boundary-layer thicknesses (at inflow) δ_0, and it has a height of about $1.2\delta_0$. Block B is about $2\delta_0$ long and is about $1.2\delta_0$ high (above the plate); the extents of block C are about $2.7\delta_0$ and $1.4\delta_0$, respectively.

By a comparison of the L_2-norms (see Table 2) of the SGS-terms in the momentum equation, the subgrid-scale stresses τ_{ij} and related terms in the energy equation are found to be dominant.

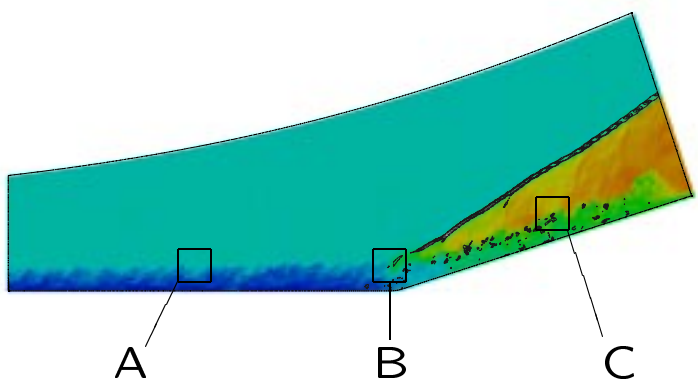

FIGURE 1. Location of subdomains for the compression corner geometry.

SGS-	L_2-norm				SGS-	L_2-norm			
term	global	A	B	C	term	global	A	B	C
$\tau_{xx} \cdot 10^3$	5.908	3.611	10.297	14.769	α_1	5.190	0.885	4.497	7.401
$\tau_{xy} \cdot 10^3$	1.330	0.424	3.124	3.143	α_2	3.255	0.694	3.329	5.535
$\tau_{xz} \cdot 10^3$	1.745	0.338	2.363	4.293	α_3	1.901	0.430	2.254	3.450
$\tau_{yy} \cdot 10^3$	2.615	0.708	5.955	6.202	α_4	0.480	0.113	0.717	1.407
$\tau_{yz} \cdot 10^3$	0.753	0.219	1.613	1.786	α_5	0.070	0.038	0.092	0.206
$\tau_{zz} \cdot 10^3$	2.512	0.507	4.637	5.149	α_6	0.114	0.127	0.181	0.229
$\frac{\partial \tau_{1j}}{\partial x_j}$	17.123	1.132	16.336	54.340	β_1	0.033	0.013	0.055	0.079
$\frac{\partial \tau_{2j}}{\partial x_j}$	4.980	1.297	9.599	12.960	β_2	0.049	0.045	0.105	0.099
$\frac{\partial \tau_{3j}}{\partial x_j}$	16.254	1.167	13.089	51.517	β_3	0.536	0.230	1.188	1.238

TABLE 2. L_2-norms of SGS-terms calculated from DNS-data.

The terms β_i (see Eq. 2) are smaller by at least a factor of 5 in subdomain A than the respective components of the divergence of the SGS-stress tensor. In the subdomains B and C the β_i are even smaller. They vanish in an isothermal flow since there $\bar{\mu} = \breve{\mu} = \mu(\tilde{T}) = const$ and accordingly $\bar{\sigma} = \breve{\sigma}$. The most significant terms in the energy equation are α_1 through α_4. The magnitude of α_5 and α_6 is about one to two orders of magnitude smaller.

In order to evaluate the performance of the models, a correlation coefficient C and a ratio A between model predictions and filtered DNS data are computed:

$$C(E,M) = \frac{\langle EM \rangle - \langle E \rangle \langle M \rangle}{\sqrt{\langle E^2 \rangle - \langle E \rangle^2} \sqrt{\langle M^2 \rangle - \langle M \rangle^2}}$$

and

$$A(E,M) = \sqrt{\frac{\langle (E(\mathbf{x}))^2 \rangle}{\langle (M(\mathbf{x}))^2 \rangle}} \quad .$$

Herein, $\langle \cdot \rangle$ denotes an average over all points of the subdomain; E is the filtered DNS data and M is the SGS model data. If C is 1, both filtered DNS and approximation are perfectly correlated. Their magnitude is the same if $A = 1$.

2.2.1 Momentum equation

In Table 3 we show A and C for τ_{ij} and α_1 for subdomain B and different subgrid models. The different models used are the Smagorinsky model with Yoshizawa's extension (Yoshizawa, 1986)

$$m_{ij} = -\overline{\rho} C_S^2 \Delta^2 \sqrt{\frac{1}{2} S_{ij} S_{ij}} \left(S_{ij} - \frac{2}{3} \delta_{ij} \frac{\partial u_k}{\partial x_k} \right) + \frac{2}{3} C_k \delta_{ij} \Delta^2 \sqrt{\frac{1}{2} S_{ij} S_{ij}}$$

$$\text{with} \quad S_{ij} = \frac{\partial u_i}{\partial x_j} + \frac{\partial u_j}{\partial x_i} \ , \quad C_S = 0.16 \quad \text{and} \quad C_k = 0.0886 \ ,$$

the dynamic mixed model (DMM, Zang *et al.*, 1993, Vreman *et al.*, 1994)

$$m_{ij} = \overline{\overline{\rho u_i}\ \overline{\rho u_j} \ / \ \overline{\rho}} - \overline{\overline{\rho u_i}}\ \overline{\overline{\rho u_j}} \ / \ \overline{\overline{\rho}} - \overline{\rho} C_d \Delta^2 \sqrt{\frac{1}{2} S_{ij} S_{ij}} \left(S_{ij} - \frac{2}{3} \delta_{ij} \frac{\partial u_k}{\partial x_k} \right)$$

where C_d is a dynamic coefficient, the scale-similarity model (SSM, Bardina *et al.*, 1983)

$$m_{ij} = \overline{\overline{\rho u_i}\ \overline{\rho u_j} \ / \ \overline{\rho}} - \overline{\overline{\rho u_i}}\ \overline{\overline{\rho u_j}} \ / \ \overline{\overline{\rho}} \ ,$$

and the resolved turbulent stresses with $r = \hat{\Delta}/\Delta = 2$ (Pruett, 1997)

$$m_{ij} = \frac{1}{r^2} \left((\overline{\rho u_i}\ \overline{\rho u_j} \ / \ \overline{\rho})\hat{} - \widehat{\overline{\rho u_i}}\ \widehat{\overline{\rho u_j}} \ / \ \hat{\overline{\rho}} \right) \quad .$$

model		τ_{xx}	τ_{xy}	τ_{xz}	τ_{yy}	τ_{yz}	τ_{zz}	α_1
Smagorinsky/	C	0.813	0.514	-0.227	0.721	-0.092	0.660	0.215
Yoshizawa	A	2.113	7.430	2.470	1.160	4.328	1.289	2.116
dynamic	C	0.947	0.850	0.696	0.849	0.578	0.695	0.592
mixed-model	A	1.481	1.364	1.055	2.186	1.542	1.827	0.934
scale-simi-	C	0.967	0.918	0.862	0.949	0.846	0.945	0.854
larity model	A	1.554	1.906	1.628	2.943	2.509	2.902	2.875
resolved	C	0.914	0.784	0.632	0.907	0.694	0.904	0.670
	A	2.872	4.731	3.326	6.509	6.775	5.961	9.515

TABLE 3. Correlation coefficient C and ratio A of the L_2-norms over subdomain B for different SGS models.

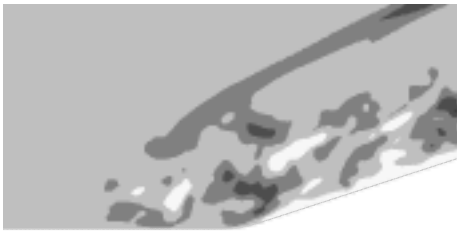

FIGURE 2A. τ_{xz}, filtered DNS data

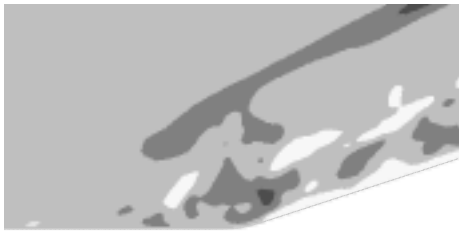

FIGURE 2B. τ_{xz}, scale - similarity model

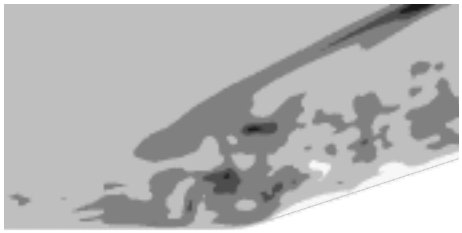

FIGURE 2C. τ_{xz}, dynamic mixed model

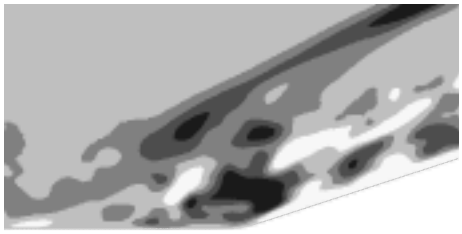

FIGURE 2D. τ_{xz}, resolved turbulent stress

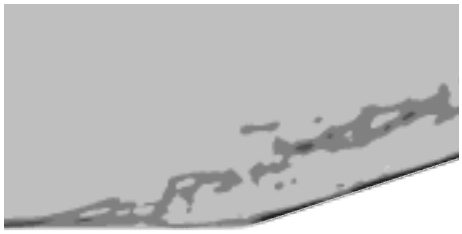

FIGURE 2E. τ_{xz}, Smagorinsky / Yoshizawa

The correlation coefficient C and the ratio A show that the Smagorinsky model correlates poorly with the filtered DNS data, see also Fig. 2E. The correlation of the turbulent resolved stresses is good for $\hat{\Delta}/\Delta = 2$ (Fig. 2D), but the magnitude is considerably under-predicted. For $\hat{\Delta}/\Delta = 1$, which coincides with the SSM, correlation and magnitude are improved (Fig. 2B). This agrees with the analytical predictions of Pruett (1997), who showed that the SSM should approximate SGS-stresses better than the turbulent resolved stresses with $\hat{\Delta}/\Delta = 2$. The DMM performs reasonably well (Fig. 2C, Table 3), but not as well as the SSM.

2.22 Energy equation

Three different models have been tested for the most significant SGS-terms of the energy equation. These models are the full dynamic mixed model (FDMM, Vreman, 1995), a scale-similarity-approach (SSM), and the resolved SGS quantities.

The SSM-approach for M_i amounts to computing the SGS-terms from the filtered variables,

$$\alpha_i = F(\mathbf{w}) \ , \qquad \beta_i = F(\mathbf{w}) \ \ ,$$

$$M_i = F(\overline{\mathbf{w}})$$
$$\text{with} \qquad \mathbf{w} = (\rho,\ \rho u,\ \rho v,\ \rho w,\ p)^T \quad .$$

The resolved SGS quantities M_i of the respective α_i are computed in the following way, using resolved and test-filtered data:

$$\alpha_i = \overline{f_i(\mathbf{w})} - f_i(\overline{\mathbf{w}}) \quad ,$$
$$M_i = \frac{1}{r^2}\left(\widehat{f_i(\overline{\mathbf{w}})} - f_i(\hat{\overline{\mathbf{w}}})\right) \quad .$$

Figure 4C shows that α_4 of the FDMM does not agree well with filtered DNS data. $\alpha_2 + \alpha_3$, as predicted by FDMM, correlates better with the filtered DNS data since it contains a scale-similarity part, Fig. 3D. The agreement between resolved SGS quantities and filtered DNS data is moderate, Fig. 3C. The SSM-approach gives much better correlation with filtered DNS data, Figs. 3B and 4B, and can furthermore provide predictions for all other SGS-terms as well, see Table 4.

model		α_2	α_3	α_4	α_5	α_6	β_1	β_2	β_3
dynamic	C	0.510		0.137	—	—	—	—	—
mixed model	A	0.762		0.628	—	—	—	—	—
scale-simi-	C	0.838	0.781	0.944	0.805	0.573	0.836	0.830	0.924
larity-model	A	3.001	2.926	5.127	2.981	0.932	3.320	1.847	3.467
resolved	C	0.330	0.552	—	—	—	—	—	—
	A	5.759	10.754	—	—	—	—	—	—

TABLE 4. Correlation coefficient C and ratio A of the L_2-norms over subdomain B for different SGS-terms of the energy equation and for β_i of the momentum equations.

3. Part 2: Treatment of shock wave

The numerical diffusion introduced by shock-capturing schemes interacts with subgrid-scale turbulence. In the recent past it has been attempted to make use of this feature by so-called MILES (monotonically integrated LES, i.e. using a monotone scheme which suppresses subgrid-scales) to model turbulent subgrid correlations, see Boris *et al.* (1992).

The question arises whether one can model non-turbulent subgrid-scales such as shocks by appropriate subgrid-scale models. This would allow for a unified approach to LES of shock-turbulence interaction similarly as with MILES but with full control of subgrid-scale modeling. Also the conservation equations could be advanced with a non-dissipative scheme such as spectral collocation or central finite-differences.

In this section, we briefly report on ongoing work on how to properly treat a shock as subgrid-scale entity in LES.

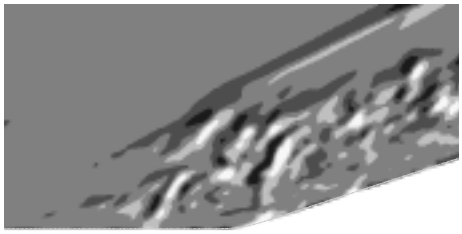

FIGURE 3A. $\alpha_2+\alpha_3$, filtered DNS data

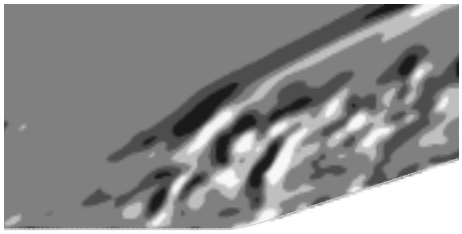

FIGURE 3B. $\alpha_2+\alpha_3$, scale-similarity model

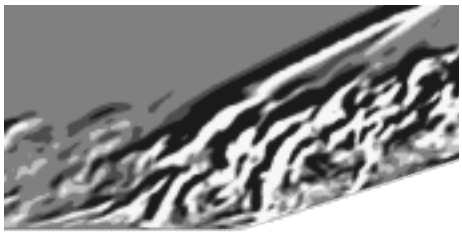

FIGURE 3C. $\alpha_2+\alpha_3$, resolved turbulent quantities

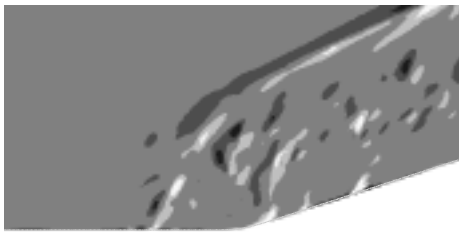

FIGURE 3D. $\alpha_2 + \alpha_3$, dynamic mixed model

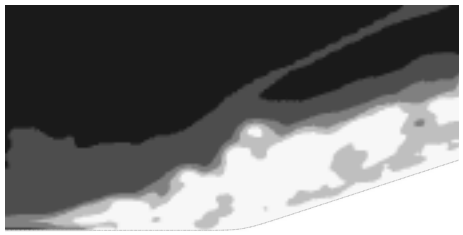

FIGURE 4A. α_4, filtered DNS data

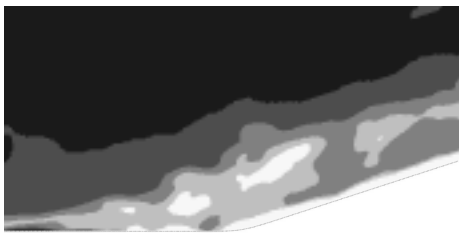

FIGURE 4B. α_4, scale - similarity model

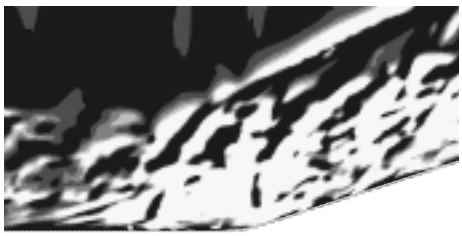

FIGURE 4C. α_4, dynamic mixed model

3.1 Shock as a sub-grid scale

If the filtering concept is interpreted strictly, then a shock, which is a discontinuity for an inviscid fluid, becomes a subgrid scale. Its resolved form can be represented by a filtered Heavyside function which is the error function. For simplicity we consider the one-dimensional filtered Euler equations

$$\frac{\partial \bar{u}}{\partial t} + \frac{\partial F(\bar{u})}{\partial x} = \mathcal{E} \tag{5}$$

with

$$\mathcal{E} = \frac{\partial F(\bar{u})}{\partial x} - \overline{\frac{\partial F(u)}{\partial x}} \tag{6}$$

where $\bar{u} = \{\bar{\rho},\ \tilde{u},\ \check{E}\}$ and $F(\bar{u}) = \{\bar{\rho}\tilde{u},\ \bar{\rho}\tilde{u}^2 + \bar{p},\ (\check{E} + \bar{p})\tilde{u}\}$. The right-hand side term $\mathcal{E}$ which is introduced by the filtering we will here call the error term. The filtered solution satisfies the modified differential Eq. (5), and $\mathcal{E}$ can have dissipative and dispersive character. If (5) could be solved exactly with an exact $\mathcal{E}$, then at any (t, x) the solution of (5) would correspond to the filtered solution of the unfiltered equation. The nonlinearity in both the filtered and the unfiltered equation is responsible for the wave steepening which generates the shock. The approximation of $\mathcal{E}$ needs be to sufficiently accurate in order to avoid that SGS-structures appear (it needs to "dissipate" the small scales generated by the nonlinearity) and to ensure the correct shock convection (it needs to compensate for the dispersive error to some extent). Concerning subgrid-scale approximation theory, a shock is a generic subgrid-scale with the advantage that one knows the exact and the filtered solution analytically.

3.2 Dynamic model

An obvious attempt is to approximate $\mathcal{E}$ by a standard SGS-model. Here we chose the dynamic Smagorinsky model since it has the basic form of a diffusion term, which benefits stabilization of the nonlinear term in Eq. (5). On the other hand it should be kept in mind that, as we have seen in Part 1, this model gives a poor approximation to $\mathcal{E}$. In our case the modeled term in the one-dimensional momentum equation is

$$m_2 = -\Delta_a C \bar{\rho} \left| \frac{\partial \tilde{u}}{\partial x} \right| \frac{\partial \tilde{u}}{\partial x}$$

and in the energy equation it is

$$m_3 = \tilde{u} \frac{\partial \bar{\rho} m_2}{\partial x} - \frac{\Delta_a^2}{(\gamma - 1) M^2} \frac{\partial}{\partial x} \left(\bar{\rho} C' \frac{\partial \tilde{u}}{\partial x} \frac{\partial \tilde{T}}{\partial x} \right) .$$

The constants C and C' are computed dynamically from a comparison with the test filtered Leonard expression for $\mathcal{E}$. Δ_a is the filter width. The main ingredients of standard dynamic modeling are the hypotheses of same SGS structure on grid and test filter levels and a dynamic constant being unaffected by the filtering. The

constants are filtered with the test filter of width Δ_b to avoid subgrid-scale contributions stemming from the ill-posedness of the coefficient-determination procedure.

Several variants of the dynamic procedure have been tried, also a form that emerges when the non-linear terms are explicitly filtered. It turned out, however, that if the explicit filtering formulation is applied consistently, terms of different character are forced to match by the dynamic procedure. A Taylor-series expansion shows that to leading order the approximation for the second component of $\mathcal{E}$,

$$L_2 \doteq \Delta_b^2 \mu_2 \bar{u}\bar{u}''$$

is forced to match

$$m_2 \doteq \Delta_a^2 \mu_2 |\bar{u}'|\bar{u}' \ ,$$

where the primes denote partial derivatives with respect to x, and μ_2 is the second moment of the filter kernel. For the generic filtered shock solution, it was shown that these terms have different character.

The test case where the model has been applied is the 1D $M = 3$ test case of Adams & Shariff (1996) without incoming perturbations. As underlying numerical schemes, an explicit 2^{nd} order finite difference scheme with 3rd order Runge-Kutta time integration and a 6th order Padé scheme (Lele, 1992) with same time integration were used. The former scheme can be stabilized by using a von Neumann-Richtmyer artificial viscosity for $\mathcal{E}$ (Hirsch, 1988) but not so the latter. None of the dynamic formulations we tried gave a stable solution of Eq. (5), so the concept of a standard dynamic model for shock computation was not pursued.

3.3 Deconvolution

From the notion that $\mathcal{E}$ can be understood not as a term to be modeled but as an error term which requires proper approximation, one can try to recover $\mathcal{E}$ by a deconvolution of the filter operation at each time instant to obtain u from $\bar{u}$. If this could be done exactly, $\mathcal{E}$ of Eq. (6) would vanish. Since a regularization of the deconvolution operation is required, a small error remains in practice. The filter used here is the same 2^{nd} order Padé filter as in section 3.2. The parameter α is chosen as $\alpha = -0.2$ in order to resemble a Gauß filter with effective width $\Delta = 4h$ (h is the grid spacing) and $\alpha = -0.43$ for $\Delta = 8h$. Note that the the smallest resolved wave number is assumed to be half the Nyquist wave number. It cannot be expected that at $\Delta = 2h$ a finite-difference scheme has any useful resolution properties and even a spectral scheme's error is of order one at this wave number.

For the abovementioned test case, a simple deconvolution by inverting the filter operation (4) has shown remarkably good agreement with filtered data obtained from a direct simulation with a high-order shock-capturing scheme, Fig. 5. Due to the ill-conditioned character of the deconvolution procedure the non-regularized deconvolution became unstable when perturbations were added to the shock-convection problem as in Adams & Shariff (1996). Indeed, the filter operation (4) is only invertible in its discretized form, a continuous Gauß filter is not invertible as can be shown by a brief argument in Fourier dual-space. Extending the work on deconvolution approaches for shock-turbulence interaction regularization procedures will be

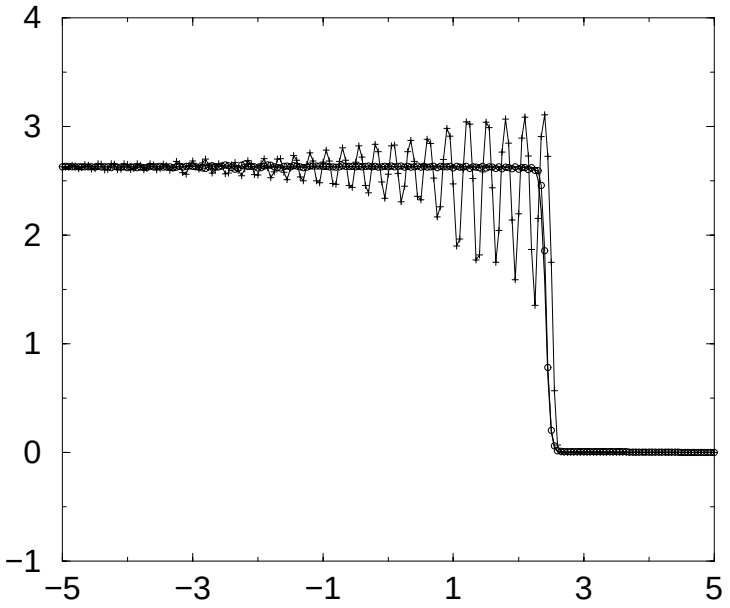

FIGURE 5. Shock simulation, velocity distribution, ——— : filtered 5th order ENO scheme, ○———○ : deconvolved 6th order Padé scheme, +———+ : artificial viscosity and 2nd order central scheme.

considered. It is expected that with regularized deconvolution methods an efficient treatment of any subgrid-scale entity, such as shocks or turbulent eddies, will be possible.

4. Concluding remarks and outlook

We have shown that standard subgrid-scale models require improvement before they can be expected to reliably represent subgrid-scale effects in physically complex flow. Nor did a straightforward application of a standard dynamic modeling procedure to treat a generic non-turbulent subgrid-scale, in our case a shock, prove to be applicable. A promising alternative appears to be (approximate) deconvolution strategies, also called de-filtering or estimation models (see the contribution of A. Domaradzki in this volume). They show in *a priori* tests a considerably higher correlation with filtered DNS data. Also often deemed misleading, in our understanding *a priori* tests constitute a necessary criterion for a SGS approximation to work, very much as a finite-difference discretization is supposed to give a good approximation to the, say, spatial derivatives in a PDE before anyone would expect that time-integration would make any sense. The traditional dynamic procedure, in fact, tries to alleviate some of these problems by making the Smagorinsky model more variable and by measuring this variability by a term of scale-similarity type (the test filtered Leonard term). The brief treatise on LES shock-treatment suggests that regularized deconvolution can be considered as a promising way for an accurate representation of subgrid-scales. It seems that many problems in the application of LES models come from the fact that LES practically always operates at the numerical resolution limits of the underlying schemes. An LES model needs

to correct what is not resolved numerically, and, obviously, then an LES model becomes related to the numerical scheme.

Acknowledgments

The first author wants to acknowledge enlightening discussions with Dr. C. D. Pruett before and during the course of this project.

REFERENCES

Adams, N. A. 1998 Direct numerical simulation of turbulent compression corner flow. *Theor. Comp. Fluid Dyn.* **12**, 109-129.

Adams, N. A., Kleiser L. 1998 Direct simulation of the turbulent boundary layer along a compression ramp at $M = 3$ and $Re_\theta = 1685$. *Report in preparation.*

Adams, N. A., Shariff, K. 1996 A high-resolution hybrid compact-ENO scheme for shock-turbulence interaction problems. *J. Comput. Phys.* **127**, 27-51.

Bardina, J., Ferziger, J. H. & Reynolds W. C. 1983 Improved turbulence models based on LES of homogeneous incompressible turbulent flows. Department of Mechanical Engineering, *Report No. TF-19*, Stanford University, Stanford, California.

Boris, J. P., Grinstein, F. F. Oran E. S. & Kolbe R. L. 1992 New insights into large-eddy simulation, *Fluid Dyn. Res.* **10**, 199-228.

Hirsch, C. 1988 Numerical Computation of Internal and External Flows. Vol. 2. *John Wiley and Sons.*

Lele, S. K. 1992 Compact Finite Difference Schemes with Spectral-like Resolution. *J. Comp. Phys.*, 103, 16-42.

Pruett, C. D. 1997 Toward Simpilification of Dynamic Subgrid-Scale Models. In *Advances in DNS / LES*, 291-298.

Vreman, B., Geurts, B. & Kuerten, H. 1994b On the formulation of the dynamic mixed subgrid-scale model. *Phys. Fluids* **6**, 4057-4059.

Vreman, B. 1995 Direct and Large-Eddy Simulation of the Compressible Turbulent Mixing Layer. Ph.D. Thesis, Dept. of. Applied Mathematics, University of Twente.

Yoshizawa, A. 1986 Statistical theory for compressible turbulent shear flows, with the application to subgrid modeling. *Phys. Fluids* **29**(7), 2152-2164.

Zang, Y., Street, R. L. & Koseff J. R. 1993 A dynamic mixed subgrid-scale model and its application to turbulent recirculating flows. *Phys. Fluids A* **5**, 3187-3196.